AIP | Journal of Applied Physics

Deep levels in a-plane, high Mg-content MgxZn1−xO epitaxial layers grown by molecular beam epitaxy

Emre Gür, G. Tabares, A. Arehart, J. M. Chauveau, A. Hierro et al.

Citation: J. Appl. Phys. **112**, 123709 (2012); doi: 10.1063/1.4769874

View online: http://dx.doi.org/10.1063/1.4769874

View Table of Contents: http://jap.aip.org/resource/1/JAPIAU/v112/i12

Published by the American Institute of Physics.

Deep levels in a-plane, high Mg-content $Mg_xZn_{1-x}O$ epitaxial layers grown by molecular beam epitaxy

Emre Gür,[1,2] G. Tabares,[3] A. Arehart,[2] J. M. Chauveau,[4,5] A. Hierro,[3] and S. A. Ringel[2,a)]
[1]*Department of Physics, Faculty of Science, Atatürk University, Erzurum 25240, Turkey*
[2]*205 Dreese Laboratory, Department of Electrical & Computer Engineering, The Ohio State University, 2015 Neil Avenue, Columbus, Ohio 43210-1272, USA*
[3]*Dpto. Ingenieria Electronica and ISOM, Universidad Politecnica de Madrid, Ciudad Universitaria s/n, 28040 Madrid, Spain*
[4]*CRHEA-CNRS, 06560 Valbonne, France*
[5]*University of Nice Sophia Antipolis, ParcValrose, 06102 Nice Cedex 2, France*

(Received 7 September 2012; accepted 19 November 2012; published online 20 December 2012)

Deep level defects in n-type unintentionally doped a-plane $Mg_xZn_{1-x}O$, grown by molecular beam epitaxy on r-plane sapphire were fully characterized using deep level optical spectroscopy (DLOS) and related methods. Four compositions of $Mg_xZn_{1-x}O$ were examined with $x = 0.31$, 0.44, 0.52, and 0.56 together with a control ZnO sample. DLOS measurements revealed the presence of five deep levels in each Mg-containing sample, having energy levels of $E_c - 1.4$ eV, 2.1 eV, 2.6 V, and $E_v + 0.3$ eV and 0.6 eV. For all Mg compositions, the activation energies of the first three states were constant with respect to the conduction band edge, whereas the latter two revealed constant activation energies with respect to the valence band edge. In contrast to the ternary materials, only three levels, at $E_c - 2.1$ eV, $E_v + 0.3$ eV, and 0.6 eV, were observed for the ZnO control sample in this systematically grown series of samples. Substantially higher concentrations of the deep levels at $E_v + 0.3$ eV and $E_c - 2.1$ eV were observed in ZnO compared to the Mg alloyed samples. Moreover, there is a general invariance of trap concentration of the $E_v + 0.3$ eV and 0.6 eV levels on Mg content, while at least and order of magnitude dependency of the $E_c - 1.4$ eV and $E_c - 2.6$ eV levels in Mg alloyed samples. © *2012 American Institute of Physics*. [http://dx.doi.org/10.1063/1.4769874]

I. INTRODUCTION

Optoelectronic devices designed to operate in the ultraviolet (UV) part of the electromagnetic spectrum, namely, UV-A (400–320 nm), UV-B (320–280 nm), and deep-UV (350–190 nm) must be based on wide bandgap semiconductor ternary alloys such as $Al_xGa_{1-x}N$ (365–200 nm) and $Mg_xZn_{1-x}O$ (368–160 nm). Although $Al_xGa_{1-x}N$-based UV emitters[1] and detectors[2] have been reported, $Mg_xZn_{1-x}O$ is an interesting alternative material system for those UV applications due to several inherent, fundamental advantages that have garnered much attention recently for potential exploitation in future technologies.[3–5] Perhaps, the most important one is the large, ~60 meV exciton binding energy present in $Mg_xZn_{1-x}O$, which is almost three times larger than that of $Al_xGa_{1-x}N$ and is independent of Mg content.[6] This gives rise to an intrinsically higher radiative recombination efficiency at room temperature, which should translate into much higher optoelectronic device efficiencies.[6] Also, the a-axis lattice parameter of $Mg_xZn_{1-x}O$ increases gradually with Mg content and the lattice mismatch between the substrate ZnO and $Mg_xZn_{1-x}O$ is very small only around ~0.20%–0.40% for $x = 0.2$–0.3, which aids the quality of quantum well and superlattice structures.[7,8] Furthermore, it has been experimentally shown that the lack of internal electric field in a-plane ZnMgO/ZnO heterostructures results in more efficient radiative recombination in quantum wells, i.e., no quantum confined Stark effect, as desired for emitter applications.[9]

Currently, work on $Mg_xZn_{1-x}O$ is in the very early stages in terms of applications of $Mg_xZn_{1-x}O$ for devices applications such as UV light emitting diodes (LEDs) and detectors.[3–5,10,11] Ultimately, as with all optoelectronic devices, the presence of various defects that can create bandgap states is of great interest since they reduce performance, hinder reliability, and lower device lifetime.[12,13] There has been recent work on trap spectroscopy of $Mg_xZn_{1-x}O$ grown by metalorganic chemical vapor deposition (MOCVD) that focused on compositional ranges from 0.056 to 0.18 in which it was found that deep acceptor-like levels having energy levels of $E_v + 0.28$ eV and $E_v + 0.58$ eV, with concentrations as high as $\sim 10^{18}$ cm^{-3}, played an important role in compensation of the electron concentration of these films.[14] The work presented here focuses on experimental characterization of deep level defects within $Mg_xZn_{1-x}O$ grown by plasma assisted molecular beam epitaxy (MBE) covering a much wider range of alloys compositions from $x = 0$ to $x = 0.56$, and bandgap energies that range from 3.36 eV for ZnO to 4.56 eV for $Mg_xZn_{1-x}O$ for $x = 0.56$.

II. EXPERIMENTAL

A systematic series of a-plane oriented, unintentionally doped (UID) $Mg_xZn_{1-x}O$ ($x = 0$, 0.31, 0.44, 0.52, and 0.56) epitaxial layers were grown by plasma assisted MBE on

a)Author to whom correspondence should be addressed. Electronic mail: ringel@ece.osu.edu. Telephone: +1 614 247 7111. Fax: +1 614 292 9562.

r-plane sapphire substrates to facilitate trap characterization via deep level optical spectroscopy (DLOS). The Mg content, its substitutional character, and the crystal structure, were previously determined in these films by Rutherford backscattering (RBS).[15] In that work, uniform growth in terms of both layers composition and atomic order as well as excellent crystal quality of the films was confirmed along with ideal substitutional behavior of Mg on Zn sublattice sites within the wurtzite lattice. Growth was initiated with a ZnO nucleation layer having a nominal thickness of 30 nm at a temperature of 400 °C, which was subsequently annealed at 600 °C for 10 min in order to obtain a smooth surface. After ZnO nucleation, the ternary $Mg_xZn_{1-x}O$ layer was grown to a thickness of 1.0 μm for each composition. Ti/Al/Ti/Au (200/1000/400/550 Å) was used as an ohmic contact, which was annealed at 400 °C. After the ohmic contact annealing, semitransparent 100 Å-thick, circular Au-Schottky contacts with a 200 μm diameter were fabricated in a coplanar geometry with respect to the ohmic contacts, to facilitate sub-bandgap light penetration for the DLOS studies. The surface underneath the Schottky contact was treated with H_2O_2 at 100 °C for 1 min before the metallization process to improve the rectification behavior.

To avoid persistent photo-conductivity effects that have been reported previously,[16] all the current-voltage (I-V), capacitance-voltage (C-V), capacitance-frequency (C-f), and DLOS measurements were performed after at least 24 h settling time in the dark. The I-V measurements were performed with a Keithley 617 electrometer. The capacitance was monitored continuously to ensure this initial condition.

All C-V and DLOS measurements were conducted at 1 kHz in order to minimize series resistance effects, which was chosen by monitoring the C-f characteristics obtained via an Agilent E4980A LCR meter. The 1 kHz DLOS measurements were conducted with a Stanford Research Systems SR830 Lock-in Amplifier. The DLOS measurements were performed using monochromatized light from quartz-tungsten halogen (QTH) and Xe lamps with photon energies between 0.5–2.0 eV and 1.2–5.0 eV, respectively, in 20 meV increments. A calibrated thermopile was used to determine the optical flux at each incident energy. DLOS measurements commenced after a thermal settling time of 80 s, to ensure thermal emission processes from shallower bandgap states were completed. A −1 V quiescent reverse bias followed by a 20 s-long, 1 V filling pulse to refill all deep levels was applied as a biasing condition in all measurements. Steady state photo-capacitance (SSPC) data were also recorded at each energy of light during the measurements. The measurements on each sample were repeated on multiple diodes on the same sample to confirm the obtained results. More details about DLOS measurements can be found in previous studies, including its application to $Mg_xZn_{1-x}O$ with lower Mg content than explored here.[14,17]

In order to accurately determine the concentrations of the traps observed in the DLOS measurements for cases where the trap concentration is an appreciable fraction (or exceeds), the background doping (i.e., the dilute concentration approximation is violated), lighted C-V (LCV) measurements were conducted with the Agilent LCR meter at 1 kHz frequency.[18] While the SSPC approach provides accurate trap concentrations in the dilute concentration limit (for $N_t < 0.1N_d$), this method underestimates the trap concentration for very high trap concentrations and LCV was found necessary for many of the traps detected in the MgZnO alloys here.[14,18]

III. RESULTS AND DISCUSSION

A. I-V, C-f, and C-V characterization of Au/$Mg_xZn_{1-x}O$ Schottky diodes

Fig. 1(a) shows the dark I-V measurements of the Au/$Mg_xZn_{1-x}O$ Schottky diodes measured at 300 K. Very low reverse leakage current density and excellent rectification behavior are observed for all compositions. The reverse dark current densities on the order of 10^{-10}–10^{-12} A/cm^2 obtained at −2 V for the highest three Mg content samples having bandgaps from 4.17 eV to 4.56 eV demonstrate significant promise for future deep UV applications, since these values of leakage currents, which typically correlate with low noise, high detectivity photo-detector devices, are more than an order of magnitude lower than earlier reports on $Mg_xZn_{1-x}O$ metal-semiconductor-metal devices.[3–5,11]

The room temperature, forward bias I-V characteristics of the Schottky diodes were numerically fitted using the standard thermionic emission theory in order to extract the diode ideality factor (n), the Schottky barrier height (Φ_b),

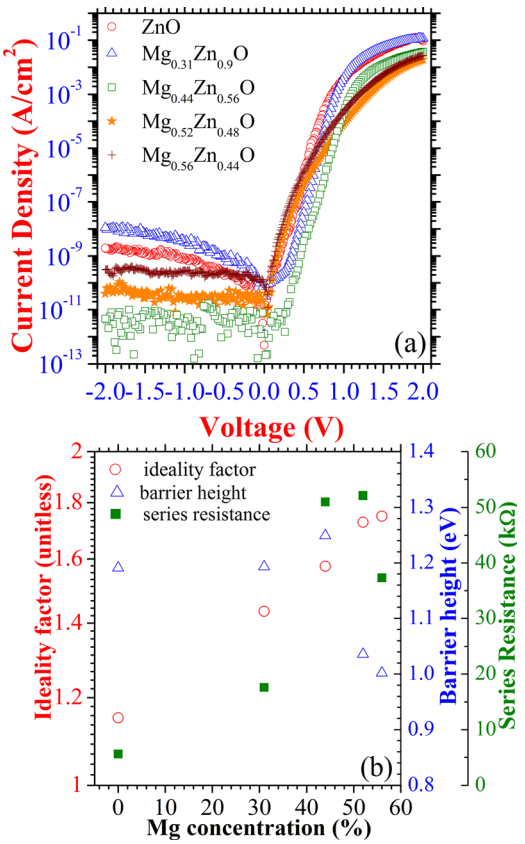

FIG. 1. (a) I-V curves performed in the dark at 300 K for the ZnO and $Mg_xZn_{1-x}O$ Schottky diodes (b) I-V transport parameters such as barrier height, ideality factor, and series resistance variation with Mg content of the Schottky diodes.

while accounting for series resistance effects (R_s), the latter of which has a clear effect on the saturation of the forward current above ~1.5 V forward bias.[19] The numerical values resulting from the fits as a function of alloy composition are compiled in Fig. 1(b). A steady increase in the value of the ideality factor from ~1.15 for pure ZnO to 1.75 for a Mg content of 56%, values which are similar to ideality factor values reported for low Mg content (up to x = 0.18) non-polar $Mg_xZn_{1-x}O$ Schottky diodes.[20] In general, barrier height values of approximately 1.0 eV were observed for all compositions from the simple I-V analysis. In addition, the R_s values of the Schottky diodes increase gradually with Mg content (except for the highest Mg content) for the same device geometry, similar to what has been reported previously in the literature.[14,20] The high series resistance of the diodes is attributed to the low net carrier concentration observed in these unintentionally doped layers (see C-V results, below) are consistent with the the coplanar device structure and the large distance between Ohmic and Schottky contact metals.

Since the trap spectroscopy measurements here are based on capacitance, accounting for the series resistance is necessary in order to extract meaningful data. The depletion capacitance will present a frequency dependence as follows:

$$C_m = \frac{C_a}{1 + (\omega R_s C_2)^2} \quad R_s G \ll 1 ,$$

where C_m is the measured capacitance, C_a is the actual capacitance, ω is the angular frequency, and G is the conductance.[21] If the series resistance is high, the term inside the parentheses becomes significant, at conventional, i.e., 1 MHz, frequencies, and as a result the measured and actual capacitance will diverge. In order to check the frequency dependence of the capacitance and to determine an appropriate frequency for subsequent capacitance measurements, the C-f characteristics were measured at room temperature in the dark between frequencies from 0.1 to 2000 kHz. Fig. 2(a) shows the C-f results at 0 V for each of the Au/$Mg_xZn_{1-x}O$ Schottky diodes. Significant frequency dispersion is observed for the Au/$Mg_xZn_{1-x}O$ diodes while no significant frequency dependence is observed for the Au/ZnO Schottky diode. As a result of the dispersion at high frequency, we chose a frequency of 1 kHz using a lock-in amplifier and/or LCR meter for subsequent capacitance-based measurements.

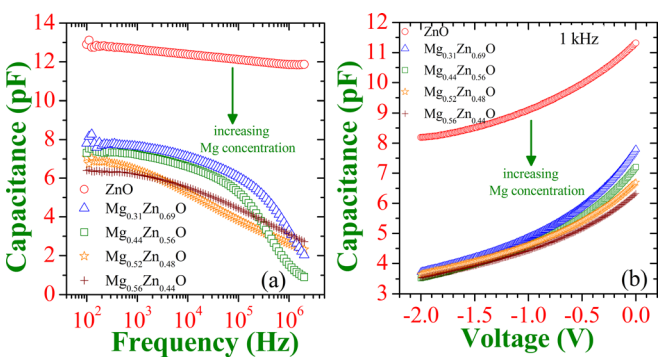

FIG. 2. (a) C-f and (b) C-V measurements performed in the dark with an LCR meter operating at 1 kHz.

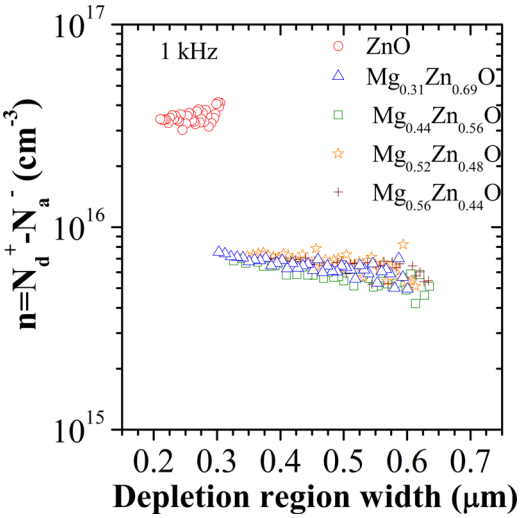

FIG. 3. (a) Net n-type doping concentration depth profile calculated from the C-V measurements shows uniform variation throughout the depletion depth for all the $Mg_xZn_{1-x}O$ samples.

Fig. 2(b) shows the C-V measurement results performed at 1 kHz on each sample. There is an immediate shift to lower capacitance values for all Mg-alloyed layers compared with ZnO. The extracted doping profiles obtained from the C-V measurements, shown in Fig. 3, reveal this to be due to almost an order of magnitude decrease in the net carrier concentration for all of the ternary alloys compared with ZnO, from $\sim 4.0 \times 10^{16}\,cm^{-3}$ for ZnO to approximately $\sim 0.6 \times 10^{16}\,cm^{-3}$ for the $Mg_xZn_{1-x}O$ alloys. The decrease may be attributed to either electron compensation by deep levels created by alloying ZnO with Mg[14,20] and/or it could be due to an increase in the donor activation energy for the $Mg_xZn_{1-x}O$ thin films due to the shift in the conduction band minimum as the Mg content increases.[22–24] In order to explore this further, DLOS and LCV measurements were performed and are discussed in Sec. III B.

B. Deep level defect characterization by DLOS and LCV

To investigate the presence of deep level defects that may exist within the wide-bandgap of the $Mg_xZn_{1-x}O$ alloy system, DLOS measurements were performed. Unlike conventional deep level transient spectroscopy (DLTS), which relies on observing thermally stimulated carrier emission from traps and thus is limited to detection of traps within approximately 1 eV of the majority carrier band edge (based on typical measurement apparatus limits), DLOS relies on optical stimulation of deep levels through sub-bandgap photoemission, as described earlier. This enables probing of levels in the n-type $Mg_xZn_{1-x}O$ bandgap anywhere from the valence band edge up to approximately $\sim E_c$-1.0 eV for all compositions, through the use of both Xe and quartz-halogen based sources. DLTS studies of shallower traps in $Mg_xZn_{1-x}O$ are the subject of ongoing work and are not discussed here.

Figs. 4(a) and 4(b) show optical cross section data extracted from DLOS transients obtained for both the Au/ZnO and the highest Mg content Au/$Mg_{0.56}Zn_{0.44}O$ Schottky

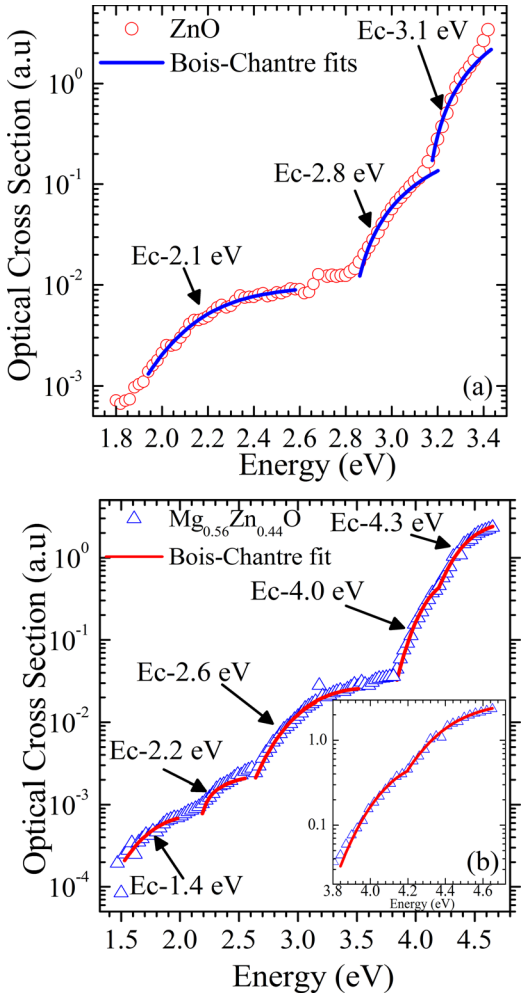

FIG. 4. Optical cross section data obtained from the DLOS transient analysis for (a) ZnO (b) $Mg_{0.56}Zn_{0.44}O$. The figure also shows the fitting of the data with the Bois-Chantre model, taking account for the Franck-Condon energy shift, if present. The inset shows the higher energy part of the spectrum in more detail with associated fitting (solid line).

diodes as representative examples of the entire sample set. The broadness of these spectra at the lower energy ranges shown is suggestive of electron-lattice coupling.[25] To account for this possibility when determining precise energy levels, the Bois-Chantre model for calculating optical cross sections from such data was employed, in which the energy associated with the lattice coupling (Franck-Condon energy) can be determined and accounted for when determining the true defect energy level.[26] Examples of such fits are also shown in Figs. 4(a) and 4(b), for ZnO and for $Mg_{0.56}Zn_{0.44}O$ Schottky diodes. Three deep levels are present in the lower half of the ZnO bandgap at $E_c - 2.1$, $E_c - 2.8$, and $E_c - 3.1$ eV, all of which were determined via the Bois-Chantre fits shown in Fig. 4(a). The associated Franck-Condon energy (d_{FC}) values for these levels are 0.5 eV, 0.2 eV, and 0.1 eV, respectively. Higher d_{FC} obtained for the $E_c - 2.1$ eV level can be seen from the broad structure of the optical cross section data in the figure for that region compared to the higher energy region of the data. In contrast to ZnO, five deep levels are revealed for the 56% Mg content Schottky diode, with energy levels of $E_c - 1.4$ eV, $E_c - 2.2$ eV, $E_c - 2.6$ eV, $E_c - 4.0$ eV, and $E_c - 4.3$ eV as shown in Fig. 4(b). In order to show clearly the need of two separate fits for the higher energy side of the optical cross section, the magnified plot for that region of energy is shown as an inset. All extracted trap energy levels as a function of MgZnO alloy composition are summarized in Table I.

A few points should be noted from the data presented in Table I. First, while three deep levels are observed in ZnO, two additional deep levels are seen with Mg incorporation, suggesting an immediate influence on carrier trapping and device characteristics for the alloys. Second, there are three deep levels whose energy levels are invariant for all alloy compositions studied here, at $\sim E5 = E_c - 1.4$ eV, $\sim E4 = E_c - 2.1$ eV, and $\sim E3 = E_c - 2.6$ eV, despite the increasing bandgap energy with the increasing Mg content (note that the E4 level is also observed in the ZnO sample). These levels effectively follow the variation in the conduction band minimum as the Mg content increases as clearly shown in Table I. Also, the Franck-Condon energy values for the E5, E4, and E3 states are invariant with Mg content, as shown in the table. Third, there are two levels whose energies are invariant with respect to the valence band maximum, at $E1 = E_v + 0.3$ eV and $E2 = E_v + 0.6$ eV, each of which presents increasing d_{FC} values with Mg content, and are common in all samples studied here. The behavior observed for E1 and E2 has been reported previously for lower Mg content samples grown by MOCVD, with almost the same energy values.[14]

With the energy levels established via the above analysis, the SSPC results can be used to obtain the concentration of each trap level observed by DLOS, which are displayed in Fig. 5. The maximum of the $\Delta C/C_0$ values observed in each

TABLE I. Extracted energy levels, E^0, referenced to the conduction band edge, and the associated Franck-Condon energies, d_{FC}, in parentheses, for each DLOS-detected state for all ZnO and $Mg_xZn_{1-x}O$ compositions studied here. The values are obtained by fitting the optical cross sections to the Bois-Chantre formalism.[26] For a few cases, the d_{FC} values could not be determined due to noise in the measurements (E5). The E3, E4, and E5 states track E_c (i.e., their energies with respect to E_c are roughly constant), whereas E1 and E2 track E_v (i.e., their energies with respect to $E_g - E^0 = E_v$ are roughly constant). All of the energy values given in the table are in eV.

	E5	E4	E3	E2		E1	
	$E^0(d_{FC})$	$E^0(d_{FC})$	$E^0(d_{FC})$	$E^0(d_{FC})$	$E_g - E^0$	$E^0(d_{FC})$	$E_g - E^0$
ZnO	…	2.1(0.5)	…	2.8(0.2)	0.6	3.1(0.1)	0.2
$Mg_{0.31}Zn_{0.69}O$	1.4	2.1(0.6)	2.6(0.3)	…	…	3.8(0.03)	0.2
$Mg_{0.44}Zn_{0.56}O$	1.5	2.1(0.4)	2.7(0.4)	3.7(0.2)	0.5	3.9(0.2)	0.3
$Mg_{0.52}Zn_{0.48}O$	1.4	2.2(0.5)	2.6(0.3)	3.9(0.5)	0.6	4.2(0.3)	0.3
$Mg_{0.56}Zn_{0.44}O$	1.4(0.3)	2.2(0.5)	2.6(0.3)	4.0(0.4)	0.5	4.3(0.6)	0.3

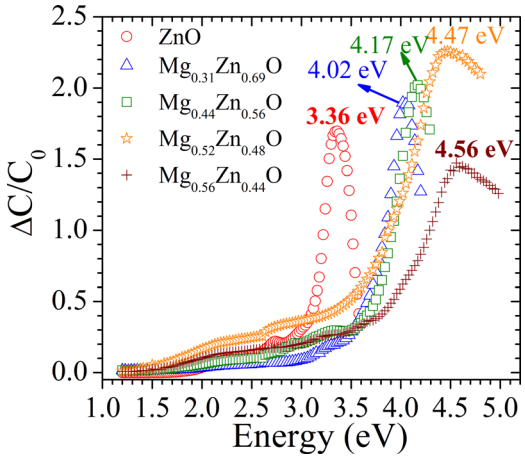

FIG. 5. SSPC data obtained for all the $Mg_xZn_{1-x}O$ samples. The peak values at high energies provide the E_g values used in the tabulated data. Note that the various SSPC steps below the bandgap are indicative of the activation of the individual traps noted in the DLOS transient fitting.

SSPC spectrum data provide the measured bandgap values for each alloy in Fig. 5, giving an experimental relationship of $E_g(Mg_xZn_{1-x}O) = 2.09x + 3.35\,eV$ for the composition range studied here. From Fig. 5, it is evident that the values of $\Delta C/C_0$ are around ~2, which means that the trap concentration is well above the dilute limit (i.e., $N_T > N_D$), for which case the SSPC provides only a lower bound to the true trap concentration. Thus, the LCV method, described earlier, was used to obtain accurate N_T values for this condition.[14,18] The LCV method monitors the difference in total depletion space charge density N using monochromatic light to selectively photo-ionize traps where N at the depletion edge x_d is extracted from the C-V profiling.[21] At each incident light photon energy $h\nu$, traps with energy $E_c - E_T < h\nu$ (for electron traps) are photo-ionized, which causes an increase in N. The difference in N for different photon energies ($h\nu_2 > h\nu_1$) at fixed x_d is the concentration of traps within that energy range ($N_T = N(h\nu_2) - N(h\nu_1)$). Selecting the photon energies of the monochromatic light using the DLOS onsets as a guide allows the concentration of each trap to be accurately determined. Fig. 6(a) shows an example of the LCV profiling data obtained for the ZnO sample. The specific illumination energies used to selectively excite the traps were chosen from both optical cross section and SSPC onset analyses. For example, the concentration of the $E5 = E_c - 1.4\,eV$ level was determined by comparing the value of N for photon energies before the onset of the next trap ($E_c - 2.1\,eV$) with N at 1.4 eV. The measurement yields an average trap concentration of $\sim 10^{15}\,cm^{-3}$ for the two highest Mg content samples. The results of the LCV analysis in terms of trap concentrations are shown in Fig. 6(b), and are summarized for each DLOS-detected level for all samples in Table II.

Interestingly, substantially higher concentrations of the E1 and E4 levels along with modestly higher (~2.5x) E2 concentrations are observed for the ZnO sample compared to all $Mg_xZn_{1-x}O$ compositions investigated here. Moreover, once Mg has been alloyed with the ZnO, there is a general invariance of trap concentration for E1 and E2. This fact, coupled with their higher concentration for ZnO implies that

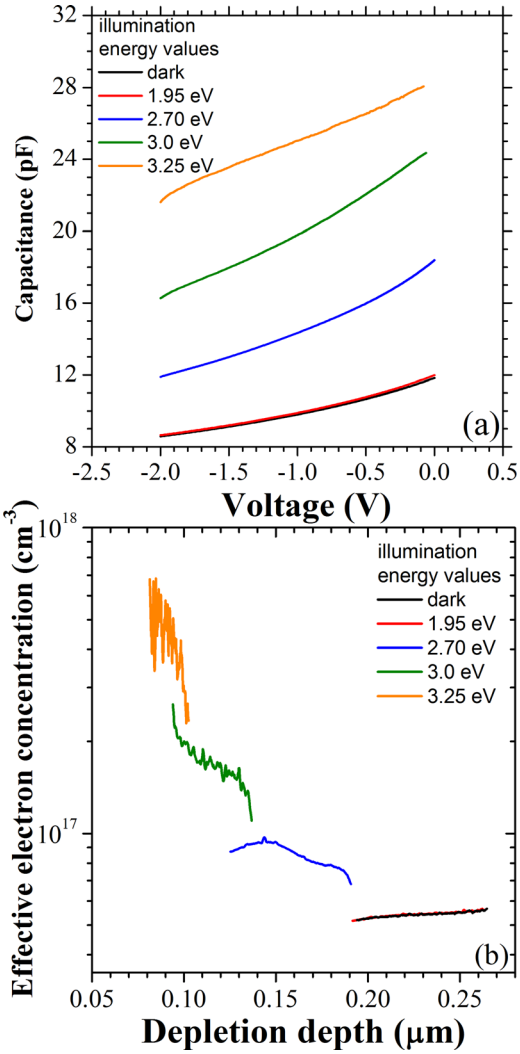

FIG. 6. LCV characterization results obtained from the ZnO sample as a representative example for all the samples characterized in this study. Figure (a) shows the actual C-V data under illumination to excite individual traps and (b) shows the net photo-ionized trap concentration for each illumination energy extracted from the LCV plots. The individual concentrations of each trap state are subsequently obtained from the step-wise differences in these concentrations and are provided in Table II.

these levels might not be associated with Mg-related defects or alloy growth issues. As for the three deep levels (E3, E4, and E5) whose energy levels follow E_c as a function of alloy composition, the general trend in concentrations is at least an order of magnitude dependency on the Mg content as shown in Table II. While the source of these levels remains unclear, separately reported RBS and high resolution x-ray diffraction on these samples do not show evidence of any phase segregation for any of the alloys studied here, and a single wurtzite structure is observed even at the highest Mg contents.[15] While a complete determination of the physical sources for the detected traps is beyond the scope of this study, this is certainly a topic deserving of attention, especially considering the mid-gap positions of these levels that would imply their importance as generation-recombination centers.

With the above comments in mind, there is some evidence to create reasonable speculation about sources. In particular, there is evidence suggesting that native point defect

TABLE II. Trap concentration, background carrier concentration, and bandgap energies for each sample as measured from LCV, C-V and SSPC, respectively.

	E_g (eV)	$n = N_d^+ - N_a^-$ (10^{16} cm^{-3})	E1 (10^{16} cm^{-3})	E2 (10^{16} cm^{-3})	E3 (10^{16} cm^{-3})	E4 (10^{16} cm^{-3})	E5 (10^{16} cm^{-3})
ZnO	3.36	3.98	39.1	8.17	…	3.310	…
$Mg_{0.31}Zn_{0.69}O$	4.02	0.64	3.0	3.02	0.08	0.039	0.009
$Mg_{0.44}Zn_{0.56}O$	4.17	0.58	3.2	3.31	0.19	0.064	0.027
$Mg_{0.52}Zn_{0.48}O$	4.47	0.62	3.8	2.24	1.50	0.130	0.140
$Mg_{0.56}Zn_{0.44}O$	4.56	0.65	2.7	1.17	1.22	0.087	0.190

sources that show acceptor-like behavior in ZnO, such as oxygen interstitials (O_i), zinc vacancies (V_{Zn}), and/or antisites such as O_{Zn}, might be related to the $E1 = E_v + 0.3$ and $E2 = E_v + 0.6$ eV levels. Among them, only the V_{Zn} energy positions in the ZnO bandgap have been theoretically calculated to be between the energies 0.18–0.30 eV for $V_{Zn}(0/-)$ and 0.34–0.87 eV for $V_{Zn}(-/--)$ above the valence band using local density calculations, in fair agreement with the experimentally determined E1 and E2 energy levels experimentally determined here.[27,28] Furthermore, V_{Zn} has the lowest formation energy among the native point defects in n-type ZnO grown in either in O-rich or Zn-rich conditions for n-type material, and prior positron annihilation studies have confirmed that a-plane, n-type ZnO contains a V_{Zn} as high as $\sim 2 \times 10^{17}$ cm^{-3}.[29,30] Interestingly, positron annihilation also revealed a slightly higher V_{Zn} concentration for $Mg_{0.06}Zn_{0.94}O$ alloys, with no evidence for Mg vacancies (noting that this is a much lower Mg content than what is being explored here).[31] Taking these findings together, and by assuming that the E1 and E2 levels are related to V_{Zn} for the MgZnO samples in this study, the higher V_{Zn} concentration in ZnO compared to $Mg_xZn_{1-x}O$ samples might be due to higher energies of formation in the alloys that result from the significantly lower Fermi level position in the bandgap resulting from the lower net doping (see Fig. 3). However, more work must be done to investigate the details of the group II vacancy in high Mg-content alloys, such as sublattice specific vacancies, which is beyond the scope of this work. Finally, the lower electron concentration that has been observed in $Mg_xZn_{1-x}O$ compared to ZnO (Fig. 2(b)) cannot be explained to result from compensation by trapping at acceptor-like states since the combined trap concentration of the levels in the lower half of the bandgap is much larger in ZnO than in $Mg_xZn_{1-x}O$. Alternatively, this lower electron concentration may be the result of an increased activation energy for the donors in $Mg_xZn_{1-x}O$ compared to ZnO, as it has been reported earlier.[22–24]

IV. CONCLUSIONS

Four a-plane high Mg content $Mg_xZn_{1-x}O$ ($x = 0.31$, 0.44, 0.52, and 0.56) samples together with a control sample ZnO were grown by plasma assisted MBE. In order to investigate the effects of the Mg incorporation on deep levels by DLOS and LCV, semi-transparent Au Schottky diodes were fabricated. I-V measurements on each Au/$Mg_xZn_{1-x}O$ devices have shown very good rectification behavior with very low reverse current density values, $\sim 10^{-10}$ A/cm^2, and a 1 eV barrier height which seems good enough for UV detector applications. DLOS measurements have shown that Mg alloying introduces two new traps compared with ZnO located at $E_c - 1.4$ and $E_c - 2.6$ eV; however, the total trap concentration determined by LCV of all traps is actually reduced compared with ZnO. The energy values for the $E1 = E_v + 0.3$ eV and $E2 = E_v + 0.6$ eV traps were found to be invariant with respect to the valence band edge, whereas $E3 = E_c - 1.4$, $E4 = E_c - 2.1$, and $E5 = E_c - 2.6$ eV were all found to be invariant with the conduction band edge in the composition range explored here. The concentration of the dominant deep levels E1 and E2 has shown no dependency to Mg content. Zinc vacancy has been suggested for the origin of $E1 = E_v + 0.3$ and $E2 = E_v + 0.6$ eV deep levels based on its reported energy position and experimentally observed high concentration. The concentration of $E5 = E_c - 1.4$ eV and $E3 = E_c - 2.6$ eV levels has shown at least an order dependency on the Mg content suggesting the Mg related origin for these levels.

ACKNOWLEDGMENTS

This work was supported by The Scientific and Technological Research Council of Turkey (TUBITAK) 2219 project program, Atatürk University long term support for scientific research, and the National Science Foundation Division of Materials Research via DMR-1106117. The work at UPM was supported by MICINN through Projects TEC2008-04718/TEC, TEC2011-28076-C02-01, and by MICINN-JST coordinated Project PIB2010JP-00279. G. Tabares was supported by the FPI-MICINN program.

[1]M. Kneissl, T. Kolbe, C. Chua, V. Kueller, N. Lobo, J. Stellmach, A. Knauer, H. Rodriguez, S. Einfeldt, Z. Yang, N. M. Johnson, and M. Weyers, Semicond. Sci. Technol. **26**(1), 014036 (2011).
[2]J. Li, M. Zhao, and X. F. Wang, Physica B **405**(3), 996 (2010).
[3]K. W. Liu, D. Z. Shen, C. X. Shan, J. Y. Zhang, D. Y. Jiang, Y. M. Zhao, B. Yao, and D. X. Zhao, J. Phys. D: Appl. Phys. **41**(12), 125104 (2008).
[4]Y. Zhao, J. Zhang, D. Jiang, C. Shan, Z. Zhang, B. Yao, D. Zhao, and D. Shen, ACS Appl. Mater. Interfaces **1**(11), 2428 (2009).
[5]Q. Zheng, F. Huang, K. Ding, J. Huang, D. Chen, Z. Zhan, and Z. Lin, Appl. Phys. Lett. **98**(22), 221112 (2011).
[6]C. W. Teng, J. F. Muth, U. Ozgur, M. J. Bergmann, H. O. Everitt, A. K. Sharma, C. Jin, and J. Narayan, Appl. Phys. Lett. **76**(8), 979 (2000).
[7]T. Makino, Y. Segawa, M. Kawasaki, A. Ohtomo, R. Shiroki, K. Tamura, T. Yasuda, and H. Koinuma, Appl. Phys. Lett. **78**(9), 1237 (2001).
[8]A. Ohtomo and A. Tsukazaki, Semicond. Sci. Technol. **20**(4), S1–S12 (2005).
[9]J. M. Chauveau, M. Laügt, P. Venneguès, M. Teisseire, B. Lo, C. Deparis, C. Morhain, and B. Vinter, Semicond. Sci. Technol. **23**(3), 035005 (2008).
[10]K. Nakahara, S. Akasaka, H. Yuji, K. Tamura, T. Fujii, Y. Nishimoto, D. Takamizu, A. Sasaki, T. Tanabe, H. Takasu, H. Amaike, T. Onuma, S. F. Chichibu, A. Tsukazaki, A. Ohtomo, and M. Kawasaki, Appl. Phys. Lett. **97**(1), 013501 (2010).

[11]G. Tabares, A. Hierro, J. M. Ulloa, A. Guzman, E. Muñoz, A. Nakamura, T. Hayashi, and J. Temmyo, Appl. Phys. Lett. **96**(10), 101112 (2010).
[12]N. Trivellin, M. Meneghini, G. Meneghesso, E. Zanoni, K. Orita, M. Yuri, T. Tanaka, and D. Ueda, Microelectron. Reliab. **49**(9–11), 1236 (2009).
[13]P. T. Lai, Z. L. Li and H. W. Choi, IEEE Photonics Technol. Lett. **21**(19) 1429 (2009).
[14]A. Hierro, G. Tabares, J. M. Ulloa, E. Muñoz, A. Nakamura, T. Hayashi, and J. Temmyo, Appl. Phys. Lett. **94**(23), 232101 (2009).
[15]A. Redondo-Cubero, A. Hierro, J.-M. Chauveau, K. Lorenz, G. Tabares, N. Franco, E. Alves, and E. Muñoz, Cryst. Eng. Comm. **14**, 1637 (2012).
[16]A. Y. Polyakov, N. B. Smirnov, A. V. Govorkov, E. A. Kozhukhova, H. S. Kim, D. P. Norton, S. J. Pearton, and A. I. Belogorokhov, Semiconductors **43**(5), 577 (2009).
[17]A. R. Arehart, C. Poblenz, J. S. Speck, and S. A. Ringel, J. Appl. Phys. **107**(5), 054518 (2010).
[18]A. Armstrong, A. R. Arehart, and S. A. Ringel, J. Appl. Phys. **97**(8) 083529 (2005).
[19]E. H. Rhoderick and R. H. Williams, *Metal-Semiconductor Contacts*, 2nd ed. (Clarendon, Oxford, New York, 1988).
[20]A. Nakamura, T. Hayashi, A. Hierro, G. Tabares, J. M. Ulloa, E. Muñoz, and J. Temmyo, Phys. Status Solidi B **247**(6), 1472–1475 (2010).
[21]D. K. Schroder, *Semiconductor Material and Device Characterization*, 3rd ed. (John Wiley & Sons, Inc., NJ, 2006).
[22]S. K. Mohanta, A. Nakamura, and J. Temmyo, J. Appl. Phys. **110**(1), 013524 (2011).
[23]A. Y. Polyakov, N. B. Smirnov, A. V. Govorkov, E. A. Kozhukhova, A. I. Belogorokhov, D. P. Norton, H. S. Kim, and S. J. Pearton, J. Electron. Mater. **39**(5), 601 (2010).
[24]Y. F. Li, B. Yao, Y. M. Lu, Z. P. Wei, Y. Q. Gai, C. J. Zheng, Z. Z. Zhang, B. H. Li, D. Z. Shen, X. W. Fan, and Z. K. Tang, Appl. Phys. Lett. **91**(23), 232115 (2007).
[25]R. Pässler, J. Appl. Phys. **96**(1), 715 (2004).
[26]A. Chantre, G. Vincent, and D. Bois, Phys. Rev. B **23**(10), 5335 (1981).
[27]A. Janotti and C. G. Van de Walle, Phys. Rev. B **76**(16), 165202 (2007).
[28]J. Li, S.-H. Wei, S.-S. Li, and J.-B. Xia, Phys. Rev. B **74**(8), 081201 (2006).
[29]F. T. A. Zubiaga, J. Zuniga-Perez, and V. Munoz-Sanjose, Acta Phys. Pol. A **114**(5), 1457 (2008).
[30]A. Zubiaga, F. Tuomisto, F. Plazaola, K. Saarinen, J. A. Garcia, J. F. Rommeluere, J. Zuñiga-Pérez, and V. Muñoz-Sanjosé, Appl. Phys. Lett. **86**(4), 042103 (2005).
[31]A. L. Yang, H. P. Song, D. C. Liang, H. Y. Wei, X. L. Liu, P. Jin, X. B. Qin, S. Y. Yang, Q. S. Zhu, and Z. G. Wang, Appl. Phys. Lett. **96**(15), 151904 (2010).